Clays and Clay Minerals, Vol. 44, No. 5, 635–651, 1996.

THE DEHYDROXYLATION OF THE KAOLINITE CLAY MINERALS USING INFRARED EMISSION SPECTROSCOPY

RAY L. FROST[1] AND ANTHONY M. VASSALLO[2]

[1] Centre for Instrumental and Developmental Chemistry, Queensland University of Technology, 2 George Street, GPO Box 2434, Brisbane Queensland 4001, Australia

[2] CSIRO Division of Coal and Energy Technology, PO Box 136, North Ryde NSW 2113, Australia

Abstract—The dehydroxylation of a series of the kaolinite clay minerals, kaolinite, halloysite and dickite, has been investigated by Fourier transform *in situ* infrared emission spectroscopy over a temperature range of 100 to 800 °C at both 50 and 5 ° intervals. Excellent correspondence was obtained between the high temperature emission spectra and FTIR absorption spectra of the quenched clay mineral phases. The major advantage of the technique lies in the ability to obtain vibrational spectroscopic information *in situ* at the elevated temperature. Dehydroxylation at a number of temperatures was determined by the loss of intensity of hydroxyl bands as indicated by intensity changes of the 3550 cm^{-1} to 3750 cm^{-1} emission spectra. As with all clay minerals, kaolinite clay mineral dehydroxylation is structure dependent. No clay phase changes occur until after dehydroxylation takes place. The kaolinite clay mineral loses the inner sheet and inner hydroxyl groups simultaneously, whereas dickite and halloysites are shown to lose the outer hydroxyls, as evidenced by the intensity loss of the ~3684 cm^{-1} peak, before the inner hydroxyl groups as determined by the intensity loss of the 3620 cm^{-1} peak. Evidence for a high temperature stable hydroxyl band at 3730 cm^{-1} for dickite and halloysite was obtained. This band is attributed to the formation of a silanol group formed during the dehydroxylation process. It is proposed that the dehydroxylation process for kaolinite takes place homogenously and involves 2 mechanisms. The dehydroxylation of dickite and halloysite takes place in steps, with the first hydroxyl loss taking place homogenously and the second inhomogenously.

Key Words—Dehydroxylation, Dickite, Emission, Halloysite, Hydroxyl, Infrared, Kandite, Kaolinite, Mechanism of dehydroxylation.

INTRODUCTION

The dehydroxylation of clay minerals is important in industry, particularly for the role of the clay mineral dehydroxylation process in oil extraction from oil shales and coals (Axelson 1987; Levy 1990; Patterson et al. 1990; Ohta and Venkatesan 1992; Levy and Hurst 1993). Dehydroxylation of the kaolinite clay minerals has been studied using a number of techniques including conductance measurements (Maiti and Freund 1981; Redfern 1987; Murata et al. 1990), diffusion (Brindley et al. 1967; Stoch and Waclawska 1981; Meinhold et al. 1992), particle sizing (Criado et al. 1986; Qiu 1992;), nuclear magnetic resonance (Lambert et al. 1989; Slade and Davies 1989; Rocha 1990; Rocha et al. 1991; Meinhold et al. 1993) and thermal analysis methods including high pressure DTA (Yeskis et al. 1985; Johnson et al. 1990; Slade et al. 1991; Chakraborty and Akshoy 1992; Guggenheim and van Groos 1992; La Iglesia 1993). Other techniques used for the elucidation of kaolinite dehydroxylation, for example neutron diffraction studies (Collins et al. 1991), X-ray diffraction (XRD) (Brindley et al. 1983; Zhang and Yuan 1993) and SEM/TEM methods (Rue and Ott 1974; Davies and Hooper 1985; Jalajakumari et al. 1989) have received less attention. Infrared spectroscopy has also proved very useful in the study of dehydroxylation (Roy 1961; Stubican and Fripiant 1963; Mackenzie 1973; Pampuch 1973; Han and Chen 1982; Tarasevich and Gribina 1985; Rocha 1990; Taranukhina et al. 1991; Kristof et al. 1993).

The generally accepted concept of kaolinite dehydroxylation results from the interaction of 2 hydroxyl groups in a two step process to form a water molecule by proton transfer leaving a chemically bonded oxygen, as a superoxide anion, in the lattice (Pampuch 1971; Maiti and Freund 1981; Brindley and Lemaitre 1987). The reaction process may be shown chemically as follows:

$$OH^- \leftrightarrow H^+ + O^{2-} \text{ and } H^+ + OH^- \leftrightarrow H_2O \quad [1]$$

These steps require proton delocalization at specific hydroxyl sites. For H_2O to form, these protons must migrate to a second hydroxyl site. If 2 adjacent hydroxyls are involved in the two-step process then this process will be homogenous (Brindley and Lemaitre 1987). If however non adjacent hydroxyls are involved, such a process would require proton diffusion (sometimes referred to as proton hopping) and probably counteractive cation diffusion with the water molecules being produced at the outer surface (Ogloza and Malhotra 1989). Where hydroxyls of different acidities are to be found, the homogenous process is more likely. It has been argued that kaolinites dehydroxylate by this homogenous process (Pampuch 1971; Brindley and Lemaitre 1987). Both infrared and conductivity measurements on layer silicates at predehydroxylation

temperatures clearly show proton delocalization taking place (Fripiat and Toussaint 1960). Electrical conductivity of kaolinite has been shown to increase up to the point where dehydroxylation takes place (White at al. 1970). Parallel infrared measurements show related changes in the infrared frequencies (White et al. 1970). Further deuterium exchange readily occurs in kaolinite at elevated but predehydroxylation temperatures, clearly providing evidence of proton delocalization (White et al. 1970). It should be noted that the majority of studies have concentrated on the dehydroxylation of kaolinite. Dickite has received little attention (Roy and Brindley 1956; Brindley and Porter 1978; Brindley and Wan 1978;) and hence no definitive mechanism for the dehydroxylation of dickite has been forthcoming. Differential thermal analysis results would suggest that the dehydroxylation of dickite is different to that of kaolinite (Holdridge and Vaughan 1957). Further, few studies have been carried out on halloysites and the assumption is generally made that the dehydroxylation of halloysite is identical to or at least similar to that of kaolinite (Holdridge and Vaughan 1957). This is an assumption that remains to be validated.

The dehydroxylation process is endothermic and the enthalpy of dehydroxlation found to be of the order of 220 kJ/mole for kaolinite (Horvath 1985; Murat et al. 1987; Petzold et al. 1989) with this dehydroxylation enthalpy dependent upon the kaolinite disorder. Similar thermodynamic values for dickite and halloysite were not readily obtained from the literature. The dehydroxylation process is not only temperature dependent but also a function of the partial pressure of H_2O and activation energies of the order of 140 to 300 kJ/mole were found (Horvath 1985). In this work, the infrared emission of the heated clay minerals is essentially carried out under the conditions of an inert atmosphere with the H_2O vapor pressure approaching zero. It could be expected that the dehydroxylation for this experiment would be similar to dehydroxylation within a vacuum. Under such conditions the dehydroxylation process, is dependent on surface conditions of the clay minerals (Toussaint et al. 1963; Brindley et al. 1967).

Clay minerals including the kandites have long been studied using infrared spectroscopy (Lazarev 1972; Farmer 1974; van der Marel 1976). Indeed, the infrared spectrum of kaolinite has been obtained over an extended temperature range (Fripiat and Toussaint 1963; Maiti and Freund 1981). For these studies the kaolinite clay minerals were diluted into a transparent host medium of KBr for absorption measurements. This is less than ideal for clay minerals due to the interaction of exchangeable cations in their structure with the alkali halide. For the kaolinite clay minerals this is less of a problem than for other clays with exchangeable cations. Furthermore, such clay samples are unsuitable for measurements at elevated temperatures as further interaction with the host is possible above 200 °C, before the halide melts at ~700 °C (Farmer 1974). Nevertheless, dehydroxylation as measured by the loss of the hydroxyl stretching vibration in the 3600 to 3700 cm^{-1} region has been reported up to predehydroxylation temperatures. Toussaint et al. (1963) reported the OH vibrational frequencies over the 40 to 400 °C range (Toussaint et al. 1963). Here it was shown that the hydroxyl frequency of kaolinite shifted from 3710 cm^{-1} at 40 °C to 3682 cm^{-1} at 400 °C. A similar result was observed by Maiti and Freund (1981) where the OH stretching vibration shifted from 3707 cm^{-1} to lower frequencies and the low frequency component at 3630 cm^{-1} shifted to higher wavenumbers. The 2 components at 3665 and 3680 cm^{-1} were observed to merge into a single band at 250 to 300 °C. Such an observation was shown in the spectra of Toussaint but not discussed. For many studies of the kaolinite dehydroxylation, the clay mineral is heated to the dehydroxylation temperature and then thermally quenched to room temperature for the appropriate measurement. This is illustrated by the FTIR spectra reported by Lambert et al. (1989) where the decrease in intensity of hydroxyl vibrational frequencies is reported as a function of weight loss. Further, dehydroxylation was interpreted in terms of changes in the lattice vibrations that occur in the 50 to 1200 cm^{-1} region. Dehydroxylation was observed by changes in the Si-O out of plane stretch at 1109 cm^{-1}, the increase in intensity of the 810 cm^{-1} band and the decrease in the intensity of the 540 to 550 cm^{-1} region attributed to the Al-O stretching of the AlO_6 octahedron. No reference was made to the decrease in the intensity of the Al-OH libration at 915 and 935 cm^{-1}.

The technique of measurement of discrete vibrational frequencies emitted by thermally excited molecules, known as Infrared Emission Spectroscopy (IES) (Vassallo et al. 1992; Frost 1995) is not widely used. The major advantages of IES are that the samples are measured *in situ* at the elevated temperature and IES requires no sample treatment other than making the clay sample a submicron particle size. This technique overcomes the difficulties associated with the use of absorbance techniques, which requires the use of pressed KBr pellets. Furthermore, the technique removes the difficulties of heating the sample to dehydroxylation temperatures and quenching before measurement since IES measures the dehydroxylation process as it is actually taking place. The benefits of the IES method are mainly that it allows samples to be studied at any temperature rather than getting the spectrum at room temperature and assuming that there is no phase change occurring as the sample cools. The IES measurement also allows kinetic studies to be carried out at any temperature based upon changes in signal intensity. The ability to run neat samples also removes the pos-

sible catalytic effects of inert diluents like KBr, which are needed for transmission measurements. We report the study of the dehydroxylation of kaolinite, dickite and halloysite using this IES technique.

THEORY

Normally when using dispersive infrared spectroscopy, the infrared beam is split into 2 beams, one for the reference beam and the other for the measuring beam. The resultant absorbance is the negative log of the ratio of the intensities of the measured to reference intensities. With FTIR, the background is measured as a single beam and the measured spectrum are a ratio to this background spectrum. In FTIR emission spectroscopy the emission spectrum is actually this single beam reference or background spectrum, modified by the instrument response function. Emission spectra were obtained as a ratio of the emission of the sample to that of a reference usually a black body source which emits a continuum of radiation according to Planck's law. Real samples will always emit less energy than that of the black body. Consequently for any given temperature, the ratio of the energy emitted by the sample to that of the black body at any given wavelength is the emissivity.

EXPERIMENTAL

Clay Mineral Samples

Clay minerals were obtained from several sources: Wards natural science establishment, Rochester, NY; The Clay Minerals Society repository (University of Missouri, Columbia, MO); and from the Australian Commonwealth Scientific and Industrial Research Organisation, Glen Osmond South Australia. Minerals were also collected from a number of Australian mineral deposits. The analysis of the minerals reported in this paper are chiefly the Clay Minerals Society standards. The minerals were dried under desiccation to remove adsorbed H_2O and were used without further purification. Samples were analyzed for phase purity using XRD techniques before infrared spectroscopic analysis.

Infrared Emission Spectroscopy

FTIR emission spectroscopy was carried out on a Digilab FTS-60A spectrometer, which was modified by replacing the IR source with an emission cell. A description of the cell and principles of the emission experiment have been published elsewhere (Vassallo et al. 1992). Approximately 0.2 mg of <0.5 μm size fractioned clay was spread as a thin layer onto a 6 mm diameter Pt surface and held in an inert atmosphere within a N_2 purged cell with an additional flow of Ar over the sample, during heating. The IES cell consists of a modified atomic absorption graphite rod furnace, which is driven by a thyristor-controlled AC power supply capable of delivering up to 150 amps at 12 volts. A Pt disk acts as a hot plate to heat the clay mineral sample and is placed on the graphite rod. An insulated 125 μm type R thermocouple was embedded inside the Pt plate in such a way that the thermocouple junction was <0.2 mm below the surface of the Pt. Temperature control of + 2 °C at the operating temperature of clay dehydroxylation was achieved by using a Eurotherm Model 808 proportional temperature controller, which was coupled to the thermocouple.

The design of the IES facility is based upon an off-axis paraboloidal mirror with a focal length of 25 mm mounted above the heater that captures the infrared radiation and directs the radiation into the spectrometer. The assembly of the heating block, and Pt hot plate is located such that the surface of the Pt is slightly above the focal point of the off-axis paraboloidal mirror. By this means, the geometry is such that approximately 3 mm diameter area is sampled by the spectrometer. The spectrometer was modified by the removal of the source assembly and mounting a gold coated mirror, which was drilled through the center to allow the passage of the laser beam. The mirror was mounted at 45° which enabled the IR radiation to be directed into the FTIR spectrometer.

Three sets of spectra were obtained: 1) the black body radiation over the temperature range selected at the various temperatures; 2) the Pt plate radiation was obtained at the same temperatures; and 3) the spectra from the Pt plate covered with the clay sample. Normally only one set of black body and Pt radiation is required. The emittance spectrum at a particular temperature was calculated by subtraction of the single beam spectrum of the Pt backplate from that of the Pt + sample, and the result was a ratio of the single beam spectrum to the black body (graphite). This spectral manipulation was carried out after all the spectral data had been collected. The spectra of a series of clays may be obtained and for the spectral manipulation, the same sets of black body and Pt hot plate radiation were used for all the clay spectra.

The emission spectra were collected at intervals of either 50 °C or 100 °C, over the range 100 to 600 °C, and then repeated on cooling at 300 and 100 °C. For 2 of the kandite clay minerals, kaolinite KGa-1 and dickite (Saint Claire), the spectra were collected at 5 °C intervals. The time between scans (while the temperature was raised to the next hold point) was approximately 100 s. It was considered that this was sufficient time for the heating block and the powdered clay sample to reach a temperature equilibrium. The spectra were acquired by co-addition of 256 scans for temperatures 100 to 300 °C with an approximate scanning time of 140 s, and 64 scans for temperatures 400 to 1200 °C, with an approximate scanning time of 45 s, with a nominal resolution of 4 cm^{-1}. Good quality spectra can be obtained providing the sample is not

https://doi.org/10.1346/CCMN.1996.0440506 Published online by Cambridge University Press

Figure 1. The IES of Kaolinite (Kga-1) over the 400 to 4000 cm^{-1} range and from 200 to 600 °C at 5 °C intervals.

too thick. If too thick a sample is used, then the spectra become difficult to interpret because of the presence of combination and overtone bands. The best quality spectra come from very thin samples of clay on the Pt plate. The success of the IES technique depends upon the temperature difference between the sample and the detector. Thus the greater the difference between the sample temperature and the detector, the better the quality of the spectrum in terms of signal to noise. Hence spectra at the lower temperatures always contain more noise. This means that the useful temperature range for the study of dehydroxlation is from 100 °C and above. The difficulty of lack of signal for the lattice region is not as pronounced. The OH region is more noisy because it is the high energy region of the spectrum. As the temperature increases more energy is available at higher wavenumbers (Planck's law), therefore at any temperature, up to about 900 °C, there is more energy at a lower wavenumber, which gives a higher signal/noise ratio. It is for this reason that the signal gets better as the temperature is increased.

Emittance values vary from 0 to 1 with a scale equivalent to an absorption spectrum. The data were linearized with respect to concentration where required, by transforming to units of $-\log 10[1 - \text{emittance}(\nu)]$. Room temperature IR absorption spectra were measured using a Digilab FTS-20/80 spectrometer, for samples dispersed in KBr disks. Spectra of 4 cm^{-1} resolution were acquired by co-addition of 64 scans. Spectral manipulation such as baseline adjustment, smoothing and normalization was performed using the Spectracalc software package (Galactic Industries Corporation, NH).

X-ray diffraction of the minerals, where necessary, was carried out on a Siemens D500 Kristalloflex diffractometer fitted with a Co tube, Si monochromator and Anton PAAR heat cameras. Heating of the sample was achieved by placing it onto a Pt strip, which lay on the diffraction circle in the camera. A current was passed through the Pt and the temperature monitored by a Pt/Pt-Rd thermocouple directly below the sample position on the underside of the Pt. Diffraction patterns were recorded from powders at 25, 400, 800, 1000, 1200 °C and then at 25 °C. The objective of the XRD studies was to check the phase changes of the clay mineral samples and to determine the crystallinity of the heated clay samples at the various temperatures during dehydroxylation. The DTA of the size fractioned clay minerals was obtained using a Setaram DTA/TGA instrument, operating at 0.5 °C/min from ambient temperatures to 900 °C.

RESULTS AND DISCUSSION

Kaolinite

The emission spectra of kaolinite (KGa-1) obtained at 5 °C intervals from 200 to 600 °C are shown in Figure 1. This figure shows a typical three-dimensional graphic of the kaolinite dehydroxylation. The numbers on the right hand side of the diagram represent the number of the spectrum. The first spectrum corresponds to 200 °C and the last spectrum to 600 °C.

https://doi.org/10.1346/CCMN.1996.0440506 Published online by Cambridge University Press

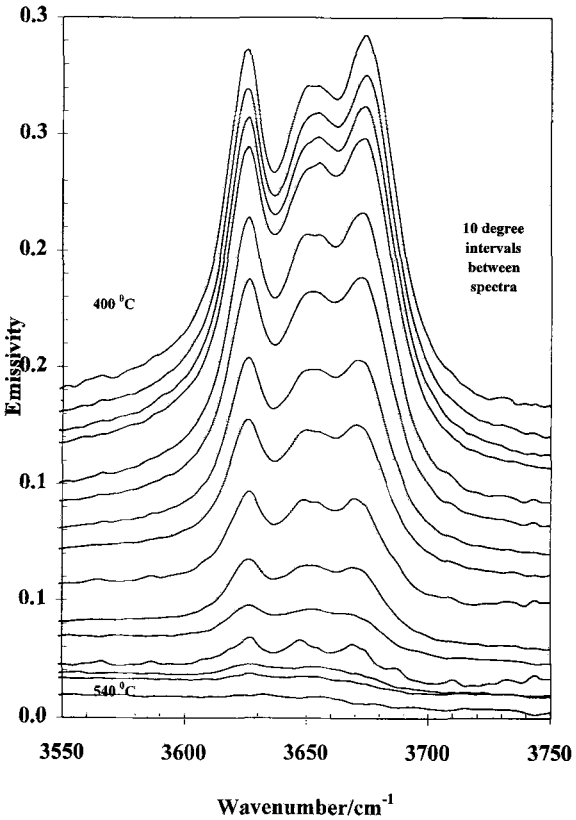

Figure 2. The IES of Kaolinite (KGa-1) over the hydroxyl stretching region 3550 to 3750 cm^{-1} and 200 to 600 °C at 10 °C intervals showing the variation of the relative intensity with temperature.

The IES spectra showing the relative intensities of the hydroxyls of kaolinite are shown (Figure 2). This figure shows the relative intensities of the hydroxyl bands over the temperature range from 400 °C to 540 °C at 10 ° intervals. This diagram clearly shows the dehydroxylation taking place over this temperature range. Water in clay minerals can be detected by the presence of the H-O-H bending mode at ~1630 cm^{-1} (Frost et al. 1995). It would appear that most of the adsorbed water has been lost by 100 °C. For clarity of presentation, the 100 °C spectrum is not shown. The experimental conditions, in which a thin layer of finely powdered clay sample is heated in an inert atmosphere is sufficient to dehydrate the samples.

Dehydroxylation as evidenced by the loss of signal due to the OH stretching modes between 3600 to 3800 cm^{-1} starts to occur between 420 and 430 °C (Figure 2). Four major bands are observed from the IES spectra of the well-ordered kaolinite KGa-1: these bands were found to be at 3686, 3664, 3649 and 3620 cm^{-1} at 175 °C. Table 2 reports the band centers of the hydroxyl bands from the infrared emission spectra of kaolinite. This table compares the values as determined by the IES method to the band center values determined by infrared absorption techniques and FT Raman spectroscopic techniques. The IES bands correspond to the four infrared absorption bands (Maiti and Freund 1981; Brindley et al. 1986; Prost et al. 1989; Frost et al. 1993) which were found at 3695, 3670, 3655 and 3621 cm^{-1} for kaolinite. Brindley et al. showed that the frequencies of these bands are dependent upon the crystallinity of the kaolinites as measured by the Hinckley indices. Prost showed that these 4 infrared absorption bands varied according to the temperature. The 4 bands were found at 3707, 3674, 3655 and 3612 cm^{-1} at 5 °K. At elevated temperatures (600 °K) the value of the 3695 room temperature band was 3677 cm^{-1} and that of the 3621 cm^{-1} band was at 3623 cm^{-1}. The 2 bands at 3670 and 3655 cm^{-1} merged into a broad profile at the elevated temperatures. FT Raman spectra were also useful for the comparison of the IES spectral positions as such bands originate from an emission technique. There was excellent agreement between the FT Raman spectra and the IES spectra for the kaolinite hydroxyl group band centers. There was also excellent correspondence between the infrared emission spectra and the corresponding absorption bands. Thus, the IES technique can be used for the *in situ* study of the kaolinite dehydroxylation at the elevated temperatures.

Table 1. Band centers for the infrared emission spectra of kaolinite hydroxyls and comparison with data from IR absorption and FT Raman spectroscopic techniques.

Band centers in cm^{-1}	IES spectra at 200 °C Kaolinite (KGa-1)	Absorption spectra at ambient temperatures (Brindley 1986)	Absorption spectra at 5K (Prost 1989)	Absorption spectra at 600K (Prost 1989)	FT Raman spectra (Frost 1995)
ν_1	3684	3695	3707	3677	3695 and 3686
ν_2	3664	3670	3674	broad	3667
ν_3	3649	3655	3655	broad	3650
ν_4	3620	3621	3612	3623	3619

In a highly ordered kaolinite such as the Georgia kaolinite KGa-1, the 4 distinct bands are assigned as follows: the 3 higher frequency vibrations (ν_1, ν_2, ν_3) are due to the 3 inner surface hydroxyls and the (fourth band at about 3620 cm^{-1} has been proved to be due to the inner hydroxyl (Johnston et al. 1990). The 3620 cm^{-1} IR band for kaolinite has been assigned to the inner hydroxyl (Ledoux and White 1964; Wada 1967; White et al. 1970; Rouxhet et al. 1977). The commonly accepted view is that the ν_1 and ν_2 bands are the coupled antisymmetric and symmetric vibrations (Brindley et al. 1986; Michaelian et al. 1987). The assignment of the ν_3 band is open to question, but the suggestion has been made that the band is due to symmetry reduction from an inner surface hydroxyl (Farmer and Russell 1964). Further, it has been shown

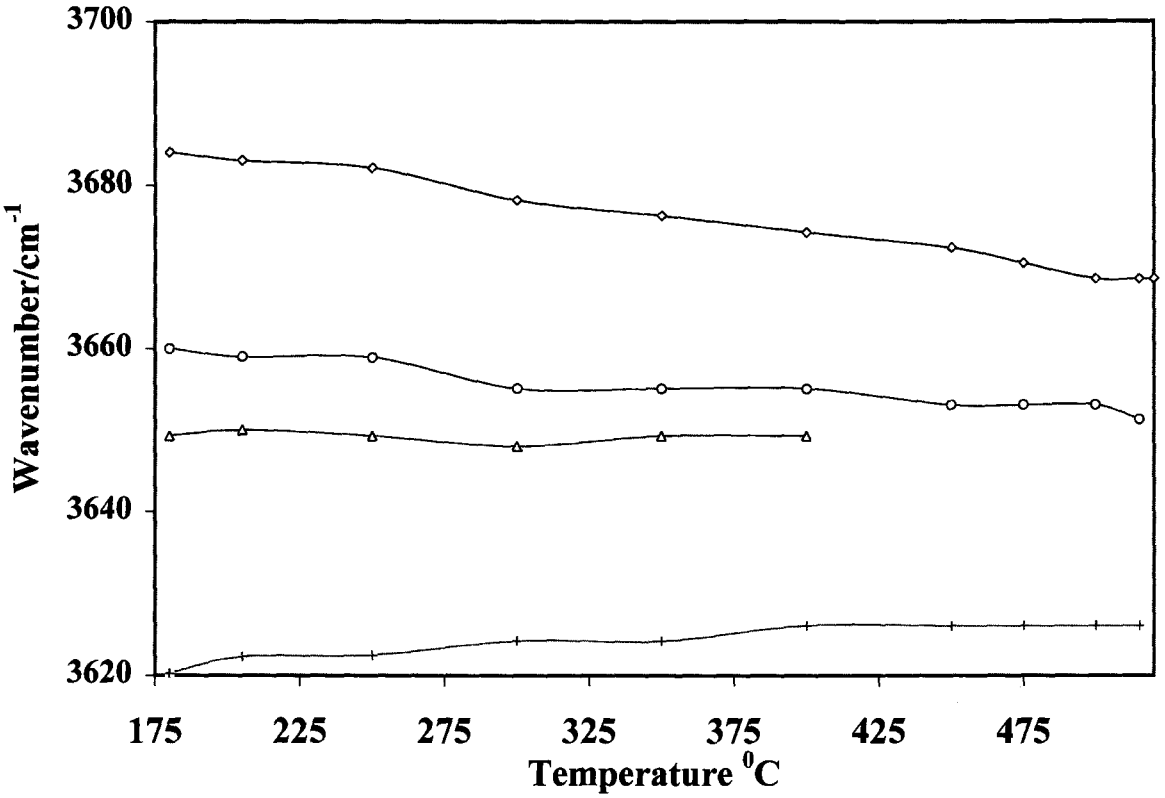

Figure 3. The Variation of the Infrared emission hydroxyl band positions with temperature.

using both Raman (Johnston et al. 1985; Pajcini and Dhamelincourt 1994) and FT-Raman spectroscopy (Frost 1995) that a fifth band at 3684 cm^{-1} exists that is also photoacoustic infrared active (Friesen and Michaelian 1986). This band has been attributed to an uncoupled inner surface hydroxyl which is not infrared active. Such a band was clearly identified in the low temperature infrared spectra of Prost et al. (1989). Prost showed by using cryogenic techniques that the infrared absorption bands were temperature dependent over the 5 to 600 °K range. Figure 3 shows the variation of peak position for the 4 hydroxyl bands as a function of temperature. The 2 middle bands coalesce into a broad profile after 375 °C. This is a similar result to the result obtained by Maiti and Freund (1981), although the temperature at which the 2 bands ν_2 and ν_3, coalesce differs. It is apparent that the reasons for the differentiation of the two peaks have been removed as the temperature is increased and serves as evidence for proton delocalization as the dehydroxylation is taking place.

Both in this work and that of Prost, all of the hydroxyl bands have been found to be temperature dependent. Prost reported that over the temperature range from 5 to 600 °K, the peak position of the inner sheet hydroxyl, ν_4, varied from 3612 to 3623 cm^{-1} (Prost et al. 1989). In this work the IES infrared peak varied from 3620 to 3626 cm^{-1} over the temperature range 175 to 520 °C at which point the intensity of the ν_4 hydroxyl approaches zero. Thus this loss of intensity indicates this inner hydroxyl has been lost. The outer hydroxyl band at 5 °K is at 3707 cm^{-1} and shifts to 3677 cm^{-1} at 600 °K in the absorption spectra of Kaolinite (Prost et al. 1989). In the IES, the outer hydroxyl peak shifted from 3670 cm^{-1} to 3655 cm^{-1} at 500 °C. Thus the band of the inner sheet hydroxyls undergoes a blue shift and the band attributed to the outer or inner sheet hydroxyl, a red shift over a wide temperature range. One possible reason for these spectral shifts can be attributed to the hydrogen bonding capacity of the hydroxyl and consequential acidity (Maiti and Freund 1981). The hydrogen bond energy of the inner surface hydroxyls decreases with increase in temperature as the inner hydroxyl protons delocalize, whereas the hydrogen bond energy of the outer hydroxyl is increasing with increased temperature. The frequency shift of the stretching modes of the external OH groups (outer or inner sheet hydroxyls), located between the layers, is larger than for the internal groups: $\Delta\nu$ for the 3670 cm^{-1} band is 16 cm^{-1} compared with $\Delta\nu$ of 4 cm^{-1} for the 3620 cm^{-1} band over the temperature range 200 to 500 °C. There is no evidence to support the proposition that the different kaolinite hydroxyls are being removed at different tem-

https://doi.org/10.1346/CCMN.1996.0440506 Published online by Cambridge University Press

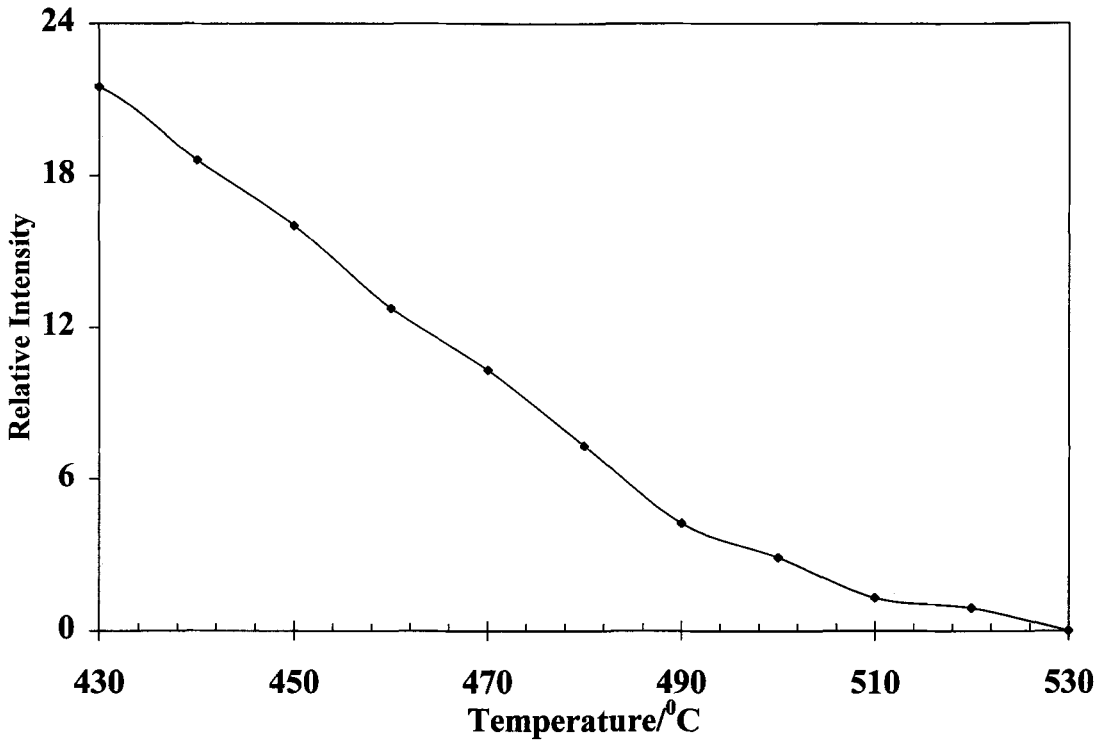

Figure 4. The Variation of the intensity of the 3620 cm^{-1} band relative to the intensity of the band at 420 °C.

peratures or at different rates. The hydroxyls are progressively lost from 420 °C and this loss is complete by 520 °C (Figure 4). It appears that the loss of the relative intensity of the 3620 cm^{-1} hydroxyl is linear over the temperature range from 420 to 480 °C. There is a change in the slope of the temperature-relative intensity graph at 480 °C until at 520 °C where there is no intensity remaining. The change in the slope would support the hypothesis that two different mechanisms are in operation for the dehydroxylation of kaolinite. The fact that differential thermal analysis (Figure 5) for the well crystalline kaolinite KGa-1 is asymmetric on the lower temperature side of the endothermic peak and shows a complex profile that supports this view. The DTA pattern shows 3 endothermic peaks centered at 480, 505 and 530 °C. These endothermic peaks support the concept that structural changes associated with the lattice are taking place as the hydroxyls are being lost. One hypothesis is that the octahedral Al sheet and the tetrahedral silica sheets are undergoing realignment after the hydroxyls are removed. It is also noteworthy that the 2 IR bands at 914 and 935.5 cm^{-1} are removed on heating at the same rate as the loss of the hydroxyls at 3500 to 3700 cm^{-1}. This is not unexpected as these 2 bands are described as inner and the outer or inner sheet AlOH librations (Farmer 1974). The 915 cm^{-1} band shifted to higher frequencies as the temperature increased; whereas the 935 cm^{-1} band did not shift. Such observations support the conclusion that the 915 cm^{-1} libration is the libration of the outer hydroxyl and that the 935 cm^{-1} libration is associated with the inner hydroxyl, which is a result reported by Prost et al. (1987) and confirmed in this work using IES.

The IES of kaolinite in the lattice region are shown in Figure 6. This figure and Figure 1 show the IES spectra as a function of temperature at 5 ° intervals. The diagram clearly shows the bands that were effected by the dehydroxylation process and those bands which remain unchanged. Figure 7 shows the relative intensities of the IES spectra of the lattice region over the dehydroxylation temperature range. The IES in the 400 to 1200 cm^{-1} region show prominent bands at 468, 541, 696, 792, 914 and 935 cm^{-1}. The corresponding absorption bands occur at 474, 540, 701, 758, 795, 916 and 938 cm^{-1} (Frost et al. 1993). Table 2 reports the IES data for the lattice modes of kaolinite and this table compares the data to the values determined by infrared absorption spectroscopy and also FT Raman spectroscopy. Good agreement is obtained between band positions obtained using the IES and FT Raman spectroscopy. There is also excellent agreement between the absorption and emission spectra of the lattice region, although some variation in the relative intensities does occur, for example, the 2 peaks at 752 and 792 cm^{-1} are weak in the absorption but more intense in the emission spectra. Also the resolution for this part of the emission spectrum is not as good as the resolution in the absorption spectrum: the

https://doi.org/10.1346/CCMN.1996.0440506 Published online by Cambridge University Press

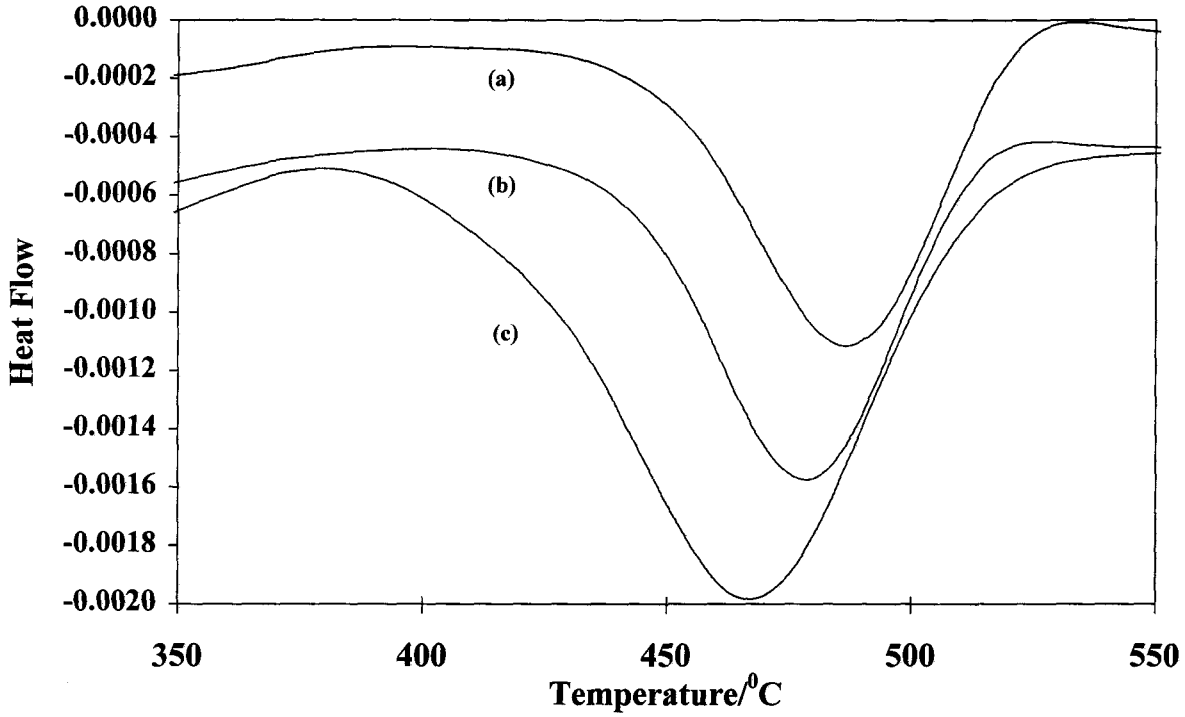

Figure 5. The DTA of the kaolinite clay mineral KGa-1, kaolinite KGa-2 and halloysite.

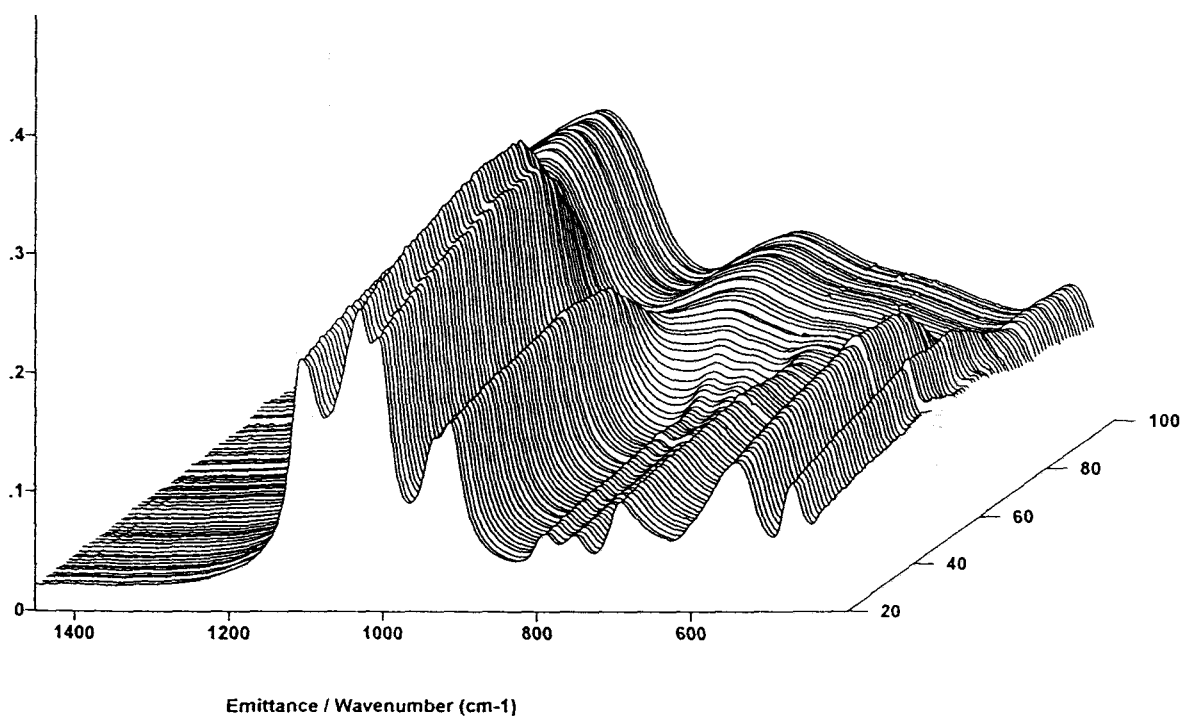

Figure 6. The IES of Kaolinite (KGa-1) lattice region over the 400 to 1400 cm^{-1} wavenumber range and from 200 to 600 °C at 5 °C intervals.

https://doi.org/10.1346/CCMN.1996.0440506 Published online by Cambridge University Press

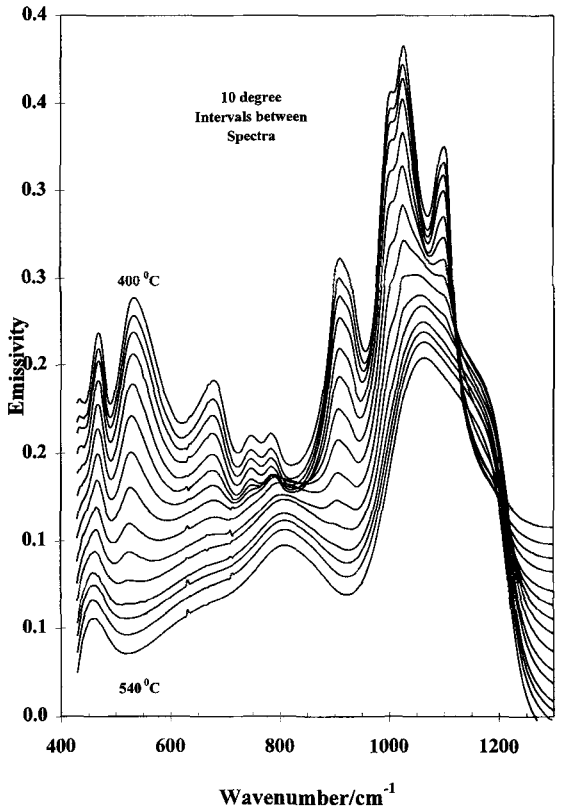

Figure 7. The IES of Kaolinite (KGa-1) lattice region over the 400 to 1400 cm^{-1} wavenumber range showing the relative intensity of the bands.

peaks at 541 and 696 cm^{-1} are very asymmetric and are not well resolved. Resolution of the bands is better using the FT Raman technique. Figures 6 and 7 assist in the assignment of the lattice vibrations of kaolinite. For example, the bands at 915 and 935 cm^{-1} are lost as dehydroxylation takes place. These bands are assigned to AlOH librations. The band at 468 cm^{-1} remains unchanged during the dehydroxylation process. This band is assigned to the SiO bending vibration. The bands at 701, 758 and 795 cm^{-1} involve OH translations in the kaolinite lattice and consequently these bands are altered as the dehydroxylation is taking place. Such observations are readily seen in Figure 6. Importantly the table clearly shows that the IES technique is very useful additional technique for determining the lattice vibrations of kaolinite and in particular at the elevated temperatures.

The spectra as illustrated in Figure 7, clearly show that no phase change takes place until the hydroxyl groups are lost as indicated by the decrease in intensity of the 935 and 914 cm^{-1} peaks and the appearance of new broad bands at 1145 and 880 cm^{-1} corresponding to the formation of dehydroxylated kaolinite sometimes referred to as metakaolinite, an amorphous phase the spectrum of which corresponds to that of mullite.

Table 2. The band centers for the lattice modes of kaolinite as measured by the IES technique and in comparison to other techniques.

Infrared emission spectroscopy	FT IR absorption (Frost 1993)	FT Raman (Frost 1993)	Probable assignment
Band centers in cm^{-1}			
468	474	475	SiO bending
		515	
541	540	560	Si-O-Al deformation
		665	Si-O-Al deformation
696	701	700	OH translation
	758	750	OH translation
792	795	790	OH translation
914	916	890	AlOH libration
935	938	940	AlOH libration

Such amorphicity of the dehydroxylated kaolinite is confirmed by X-ray analysis at the elevated temperatures. The band at 468 cm^{-1} remains unchanged through the heat treatment of the kaolinite apart from the normal red shift. This band has been attributed to the Si-O asymmetric band. The intensity of the other bands (541, 696, 792, 914 and 935 cm^{-1}) all change on heating and the intensity loss is related to the dehydroxylation. The 541 cm^{-1} band has been attributed to the Si-O-Al in plane bend; this bend is altered on the thermal treatment of the clay mineral and is lost at the elevated temperatures. The other intense emission bands occurring at 1007, 1032 and 1110 cm^{-1} are all Si-O stretching modes. These bands change into the mullite spectrum on heating above 520 °C.

Dickite

Dickite and kaolinite have the same stacking of layer sequences. Each layer is shifted by $-a_1/3$. Crystals are held together by hydrogen bonds formed between adjacent layers. The OH groups of the gibbsite layers form hydrogen bonds to the oxygen atoms of the adjacent silica layers (Brindley 1976). The space group for dickite is Cc with the position of the octahedral site in dickite alternating between B and C sites in successive octahedral sheets (Johnston et al. 1990).

The IES of the hydroxyl region of the San Juanito and Sainte Claire dickites are shown in Figures 8 and 9. Table 3 shows the band positions of the dickite hydroxyls and compares these positions with those values determined by IR absorption and FT Raman techniques. Three hydroxyl bands are observed at 200 °C, at 3622, 3660 and 3700 cm^{-1}. The assignment of these hydroxyls is similar to that of kaolinite where the peak at 3700 cm^{-1} is ascribed to the outer sheet hydroxyl and the 3622 cm^{-1} peak to the inner sheet hydroxyl. In the KBr absorption bands for Wisconsin dickite, 3 components at 3618, 3650 and 3700 cm^{-1} were observed at 300 °K (Farmer and Russell 1964; Prost et al. 1987). The peak positions from the IES of dickite

https://doi.org/10.1346/CCMN.1996.0440506 Published online by Cambridge University Press

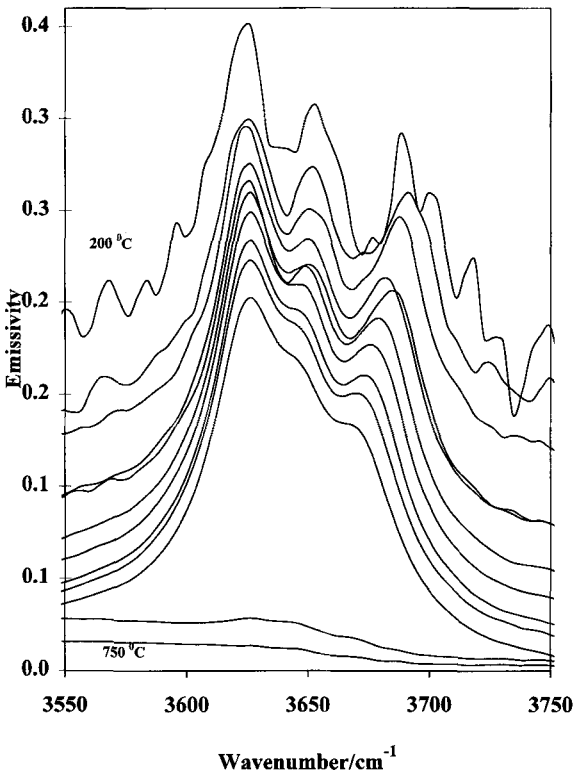

Figure 8. The Infrared emission spectra of the San Juanito Dickite hydroxyl region for the 400 to 4000 cm^{-1} region over the temperature range 200 to 750 °C at 50 °C intervals.

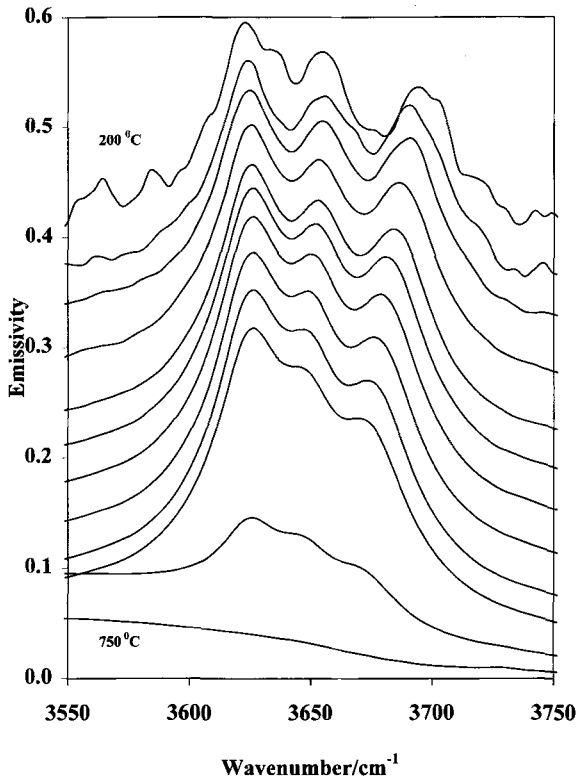

Figure 9. The Infrared emission spectra of the Sainte Claire Dickite for the Hydroxyl stretching region over the temperature range 200 to 750 °C.

hydroxyls correspond well with the positions of the 327 °C absorption spectra where peaks were found at 3622, 3652 and 3683 cm^{-1} (Prost et al. 1989). Large changes are observed for the frequency of the external hydroxyl groups similar to that effect for kaolinite: The $\Delta\nu$ for the 3700 cm^{-1} peak is 30 cm^{-1} over the temperature range 200 to 650 °C. Such a large variation in the peak position of the 3700 cm^{-1} hydroxyl was also found for the Sainte Claire dickite over the temperature range 5 to 350 °K, where this peak varied linearly from 3732 cm^{-1} at 18 K to 3708 cm^{-1} at 300 °K (Bish and Johnston 1993). Such a blue shift for the 3700 cm^{-1} peak can be attributed to the decrease in the isolation of the Al-OH groups as dehydroxylation is taking place.

Almost no variation in the wavelength of the IES 3622 cm^{-1} peak was observed over the dehydroxylation temperature range [$\Delta\nu$ = 4 cm^{-1}]. Whereas with kaolinite, the inner surface hydroxyl at 3620 cm^{-1} showed a blue shift, the corresponding peak in dickite showed almost no shift. A similar result was observed in the absorbance infrared spectra of Sainte Claire dickite where the 3619 cm^{-1} band position shifted from 3619.4 cm^{-1} at 18 °K to 3622.3 at 300 °K (Bish and Johnston 1993). The 3622 cm^{-1} peak at 600 °K was observed to shift to 3615 cm^{-1} at 5 °K (Prost et al. 1989). The fact that the 3620 cm^{-1} peak is almost independent of temperature is consistent with minimal change for the overall structure as the hydroxyl groups are removed. The absorbance spectrum of the outer hydroxyl showed a peak at 3683 cm^{-1} at 600 °K, which shifted to 3711 cm^{-1} at 5 °K (Prost et al. 1989). It should be noted that the outer hydroxyl band at 5 °K was split into several components at 3726, 3711 and 3685 cm^{-1}. This difference in the peak shift between the hydroxyls of kaolinite and dickite may be

Table 3. Band centers for the infrared emission spectra of dickite hydroxyls and comparison with data from IR absorption and FT Raman spectroscopic techniques.

Dickite	IES spectra at 200 °C	FTIR absorption spectra at ambient temperatures (Frost 1993)	Absorption spectra at 5K (Bish 1993)	Absorption spectra at 600K (Prost 1989)	FT Raman spectra (Frost 1995)
		Band centers in cm^{-1}			
			3731		
ν_1	3700	3704	3717	3683	3703
		3681	3691		
ν_2	3660	3654	3655	3652	3652
					3639
ν_3	3622	3621	3619	3622	3621

https://doi.org/10.1346/CCMN.1996.0440506 Published online by Cambridge University Press

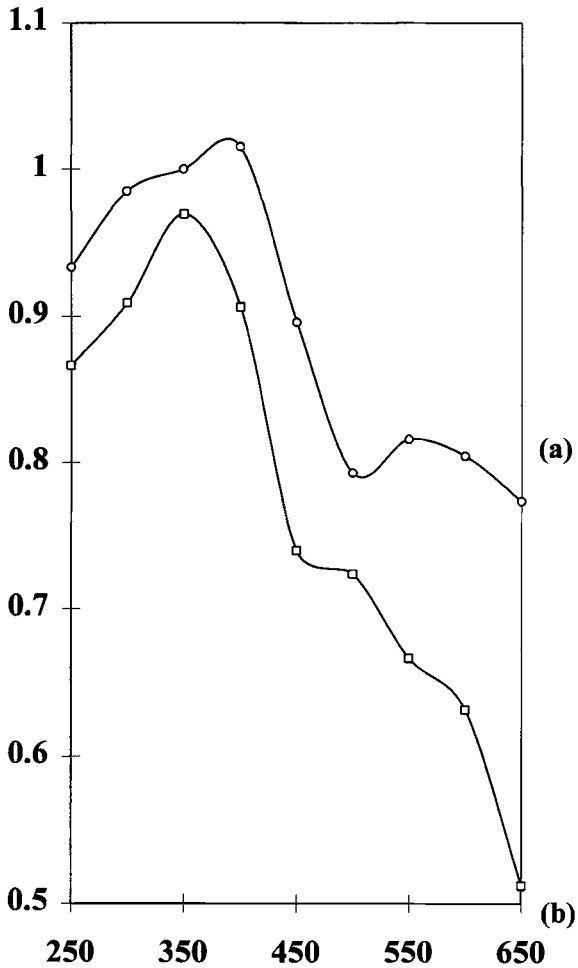

Figure 10. Variation of the relative intensity of the 3700 and 3660 cm^{-1} bands of dickite relative to the 3622 cm^{-1} band of dickite.

attributed to the differences in the H bonding of the inner surface hydroxyl groups. The interlayer H bonding is weaker in dickite and the H bonding for the inner surface hydroxyls is unchanged by thermal treatment (Brindley et al. 1986). The outer hydroxyl for both minerals shows a strong red shift. The intensity of the hydroxyls starts to diminish at 475 °C and there is no intensity remaining by 700 °C. This indicates the temperature range over which dehydroxylation occurs. Figure 10 illustrates the relative intensity of the 3700 and 3660 cm^{-1} bands relative to the intensity of the 3622 cm^{-1} band. Both bands decrease in intensity compared to the 3622 cm^{-1} band, thus indicating that the outer hydroxyls are dehydroxylating first and that not all of the hydroxyls are simultaneously removed from the dickite clay. The slope changes of the relative intensity-temperature plots support the view that more than one mechanism is operating in the dehydroxylation of dickite. Indeed the increase in intensity over the predehydroxylation temperature range (250 to 350 °C) is indicative of increased proton delocalization. The slope changes are indicative of a second mechanism of dehydroxylation taking place.

The DTA patterns of the 2 dickites studied in this work are shown in Figure 11. DTA experiments for these dickites show several components in the endotherm of dickite. The DTA pattern for the San Juanito dickite clearly shows several endotherms at 500, 560, 640 and 720 °C. The endotherm at 500 °C is in a similar position to that for kaolinite and hence is attributed to the dehydroxylation of kaolinite lattice like particles in the dickite. The 560 °C endotherm is attributed to the outer hydroxyl, the 640 °C endotherm to the inner hydroxyls and the broad endotherm at 720 °C to the non hydrogen bonded hydroxyls evidenced by the high frequency peak at 3730 cm^{-1}. This doubling of the endotherm has been previously interpreted as being caused by the dehydroxylation of the outer OH groups of the external structural layers (Stoch 1964). Therefore, it was concluded that the dehydroxylation of dickite is different to that of kaolinite in that not only are the hydroxyl groups lost at different rates, but different mechanisms are likely. The first step in the mechanism of dehydroxylation is the dissociation of a hydroxyl group to a free proton and an oxygen ion, while the second step is the combination of the free proton with a second hydroxyl group to form H_2O. The reaction may be considered to be homogenous if these 2 reactions in the mechanism involve 2 adjacent hydroxyl groups of different acidity (Pamuch 1971). For kaolinite, this work supports the view that both types of hydroxyl groups are lost homogenously. If the protons produced diffuse to more favorable reaction sites, then this type of mechanism of dehydroxylation may be described as heterogenous or inhomogeneous (Ball and Taylor 1961; Brindley 1961, 1963). Since the outer hydroxyl is being lost at a different rate to the inner hydroxyl, one possibility for dickite is that the outer hydroxyl is lost by an homogenous mechanism and the inner hydroxyl by a heterogenous mechanism. It is noteworthy that, as the dehydroxylation is taking place, the IES spectra show a very broad band centered at 3500 cm^{-1}. This is attributed to the water produced in the mechanism discussed above. No such feature was observed in the kaolinite spectra. It is probable that the diffusion of the water in the dickite structure is slow. There is also evidence (Figure 9) that some new hydroxyl band is formed at 3730 cm^{-1} and is retained until higher temperatures (750 °C). Therefore, the intensity of this band is weak and the band may be attributed to isolated hydroxyl groups that are locked within the structure and require the inhomogeneous mechanism for dehydroxylation. Such a band is typical of a silanol group. The formation of an SiOH group is further evidence that dickite dehydroxylation is taking place through an inhomogeneous mechanism

https://doi.org/10.1346/CCMN.1996.0440506 Published online by Cambridge University Press

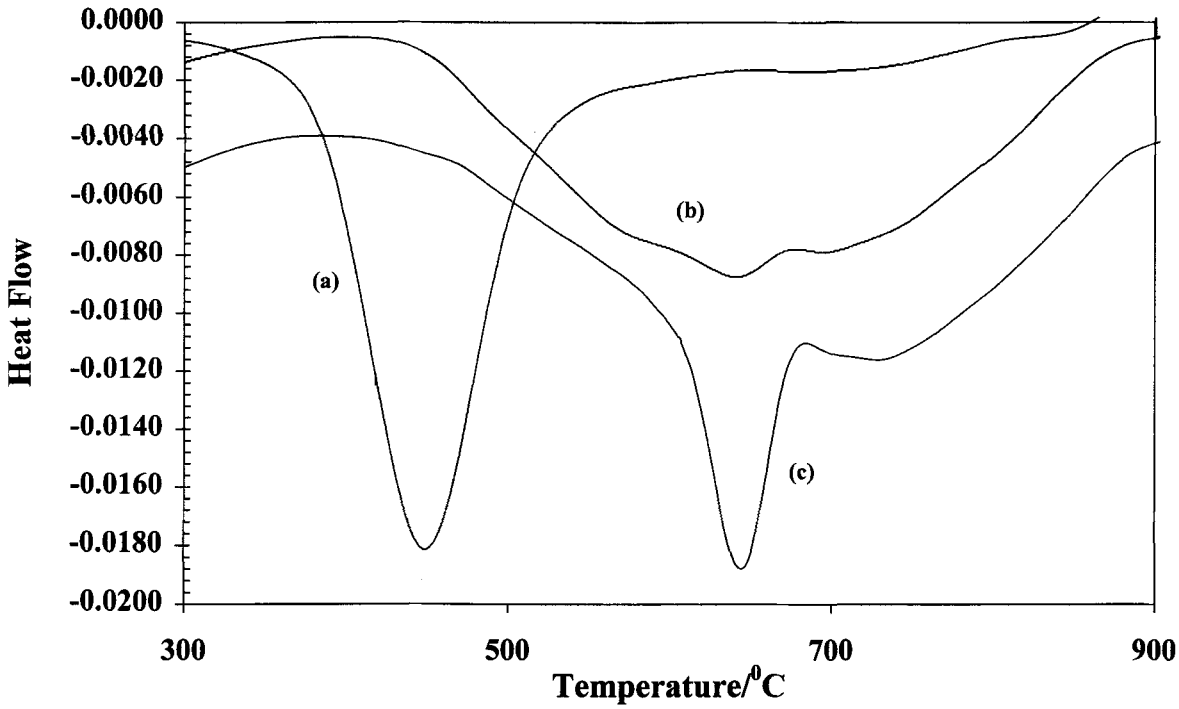

Figure 11. The DTA of kaolinite, San Juanito Dickite and Sainte Claire Dickite.

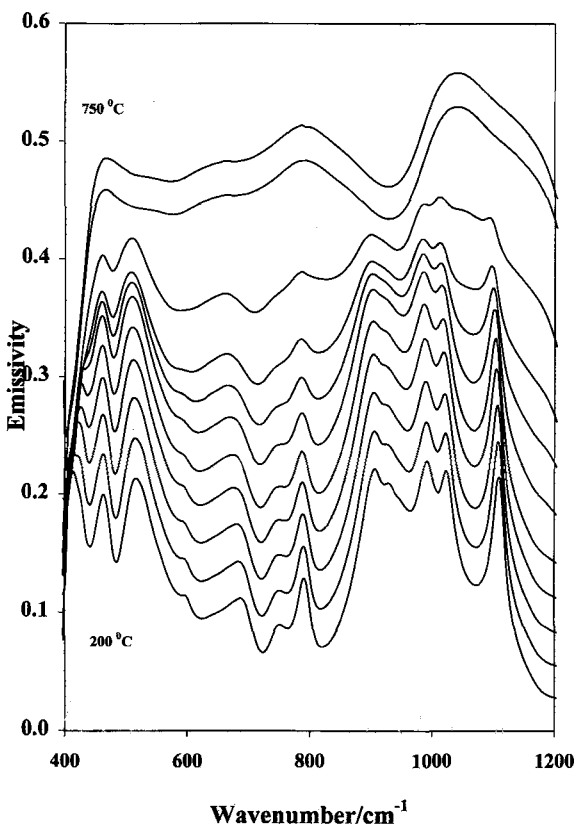

Figure 12. The IES of the lattice region of San Juanito Dickite over the temperature range 200 to 750 °C.

involving the transfer of OH groups from the Al to the Si during the dehydroxylation process. An alternative consideration would be that the silanol groups were always present in the dickite structure, but in very low concentrations and are not easily observed until the Al hydroxyl groups were lost. Such a consideration is unlikely. It is worthwhile comparing this peak to the 3726 cm^{-1} peak reported by Prost in the dickite spectrum at 5 °K (Prost et al. 1989). For the latter case, the cryogenic technique enabled the resolution of the 3726 cm^{-1} peak; whereas in the IES, the peak could not be observed until the loss of the hydroxyls allowed the observation of this 3730 cm^{-1} peak.

Figure 12 shows the IES of the San Juanito dickite in the lattice region are shown in Figure 12. Table 4 reports the spectral data for the lattice modes of dickite. This table also draws a comparison between the IES data and the data as determined by FTIR absorption techniques and FT Raman spectroscopic techniques. The major infrared emission peaks in the 400 to 1200 cm^{-1} region of dickite at 200 °C occur at 412, 460, 515, 697, 745, 790, 895, 998, 1022 and 1110 cm^{-1}. The corresponding peaks in the absorption spectrum occur at 423, 468, 534, 696, 755, 794, 1000, 1033 and 1133 cm^{-1}. Peaks in the FT Raman spectra of these clays have been reported (Frost et al. 1993). Consequently there is excellent agreement between the emission and absorption spectra. As the temperature is increased over the temperature range 0 to 750 °C, the

https://doi.org/10.1346/CCMN.1996.0440506 Published online by Cambridge University Press

Table 4. The infrared emission spectral data for the lattice modes of San Juanito Dickite and comparison with the data from FTIR absorption and FT Raman spectroscopic techniques.

Infrared emission spectroscopy of dickite	FT IR absorption (Frost 1993)	FT Raman (Frost 1993)	Probable assignment
	Band centers in cm^{-1}		
412	423		
460	468	480	SiO bending
515		515	
	534	560	Si-O-Al deformation
		665	Si-O-Al deformation
697	696	710	OH translation
745	755	750	OH translation
790	794	790	OH translation
895	912	910	AlOH libration
	935		
998	1000		
1022	1033	1025	SiO stretch
1110	1118	1080	SiO stretch

spectral peaks undergo a red shift of 16 cm^{-1}. For example, the SiO asymmetric stretching peak is at 1110 at 200 °C and is at 1094 cm^{-1} at 600 °C before the phase change to mullite takes place. The broad peaks at 685 and 790 cm^{-1} together with the sharper peak at 460 cm^{-1} are retained in the same positions from the dehydroxylating dickite structure through to the mullite phase. The 677 cm^{-1} peak has been assigned to the AlO stretching frequency (Rouxhet et al. 1977) and the 460 cm^{-1} band has been assigned to an in plane Si-O-Si bend. Thus, these assignments explain the retention of the peaks in these positions through the dehydroxylation process.

Halloysites

Halloysite, one of the polymorphs in the kaolinite series, differs from kaolinite and dickite in that the unit kaolinite layers are present but are displaced along the a and b axes in a random fashion. Halloysite exists in both a 7 Å and 10 Å form. Since there is no H bonding between successive units as occurs with kaolinite and dickite, halloysite structure is penetrable by water to form the hydrated, 10 Å structure. This structure readily loses water at temperatures above ambient to form the 7 Å halloysite, the metahalloysite which has the same empirical formula as kaolinite. The 7 Å halloysite polymorph was analyzed by infrared emission techniques.

Infrared emission spectra of the hydroxyl region of the 2 halloysites studied are shown in Figures 12 and 13. The band centers for the halloysite hydroxyl groups are reported in Table 5. This table also compares the data as determined by infrared absorption, FTIR absorption and FT Raman spectroscopic techniques. For the 'Eureka' halloysite, it is clearly observed that the outer hydroxyl group at 3680 cm^{-1} is lost before the inner hydroxyl group at 3628 cm^{-1} (Figure 12). For the New Zealand halloysite, this loss is not as easily observed. As with kaolinite, the 3680 cm^{-1} peak exhibited a temperature dependence with a shift in peak frequency of 16 cm^{-1} over the 200 to 500 °C temperature range. Between 400 and 600 °C the outer halloysite hydroxyl was lost and at the same time, as with dickite, there was evidence that a new high temperature hydroxyl peak appears at 3730 cm^{-1}. A similar peak was observed in the dehydroxylation

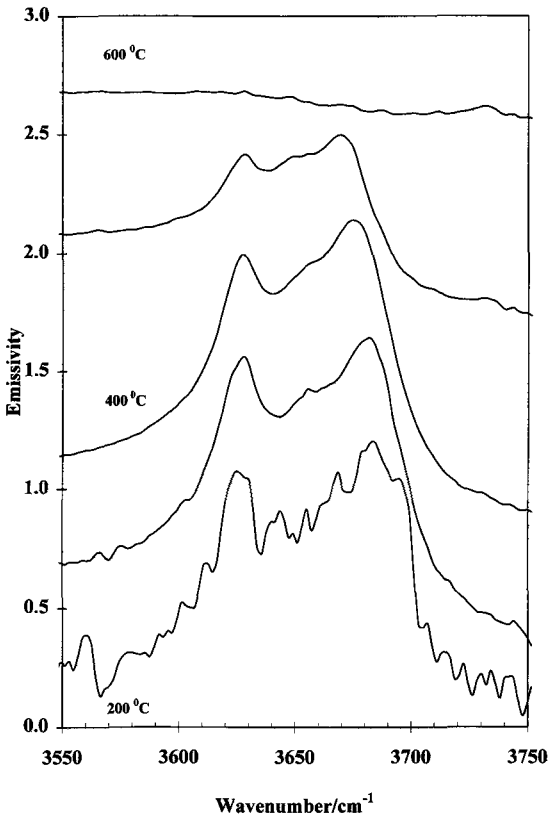

Figure 13. The IES of New Zealand Halloysite hydroxyls over the 200 to 600 °C range.

Table 5. The infrared emission spectral data for the halloysite hydroxyls and comparison with the data as determined by infrared and FTIR absorption techniques and FT Raman spectroscopic techniques.

Band centers in cm^{-1}	IES spectra at 200 °C	FT IR absorption spectra (Frost 1993)	IR absorption spectra (Van der Marel 1969)	FT Raman spectra (Frost 1995)
ν_1	3680	3695	3695	3698 and 3680
ν_2	3670	3670	3668	3660
ν_3	3650	3655	3652	3630
ν_4	3628	3620	3624	3622
		3602		

https://doi.org/10.1346/CCMN.1996.0440506 Published online by Cambridge University Press

Table 6. The infrared emission spectral data for halloysite and comparison with the spectral data obtained from FTIR absorption and FT Raman techniques.

Infrared emission spectroscopy of Halloysite	FT-IR absorption (Frost 1993)	FT Raman (Frost 1993)	Probable Assignment
Band centers in cm^{-1}			
		425	
	434	440	
		465	
470	474	470	SiO bending
		510	
540	540	550	Si-O-Al deformation
		635	Si-O-Al deformation
696	690	710	OH translation
	752	750	OH translation
792	790	790	OH translation
914	911	910	AlOH libration
935	938	940	AlOH libration
1015	1013		SiO stretch
1036	1032		SiO stretch
1110	1090	1110	SiO stretch

of montmorillonites (Frost 1995) where a peak at 3728 cm^{-1} was found. It is probable that such a peak results from hydroxyl groups that were not hydrogen bonded and as with dickite, was attributed to the formation of a silanol group formed during the dehydroxylation process. The DTA pattern of halloysite (Figure 9) shows one major endotherm, which is strongly asymmetric with the dehydroxylation starting at lower temperatures than with the kaolinites.

The IES spectra for the lattice region of halloysite are shown in Figure 12. Table 6 reports the IES spectral data for halloysite and draws a comparison between the IES spectral data and the data obtained by FTIR absorption and FT Raman spectroscopic techniques. The bands such as the 430 cm^{-1} band are retained in the same peak position throughout the thermal transformation process whereas the 540 cm^{-1} band is lost during dehydroxylation. The 430 cm^{-1} band has been assigned to an Si-O-Si bending vibration (Farmer 1974) and the 540 cm^{-1} IES band is attributable to the in-plain Si-O-Al bend. This vibrational mode is lost upon the thermal destruction of the lattice. A similar argument can be made with respect to the 790 cm^{-1} band that remains unchanged upon heating and to the 910 cm^{-1} band that has been attributed to the Al-OH libration, which is lost during dehydroxylation.

Since H bonding between successive halloysite layers does not occur, it could be predicted that halloysite dehydroxylation would be different to that of kaolinite. The hypothesis that the outer hydroxyls are removed homogenously is tenable, as these dehydroxylate first and at a different rate than that of the inner hydroxyl. The observation that some new hydroxyl group with a band position at 3730 cm^{-1} is found, which due to its peak position is not H bonded, leads to the proposition that this dehydroxylation of halloysite is inhomogeneous.

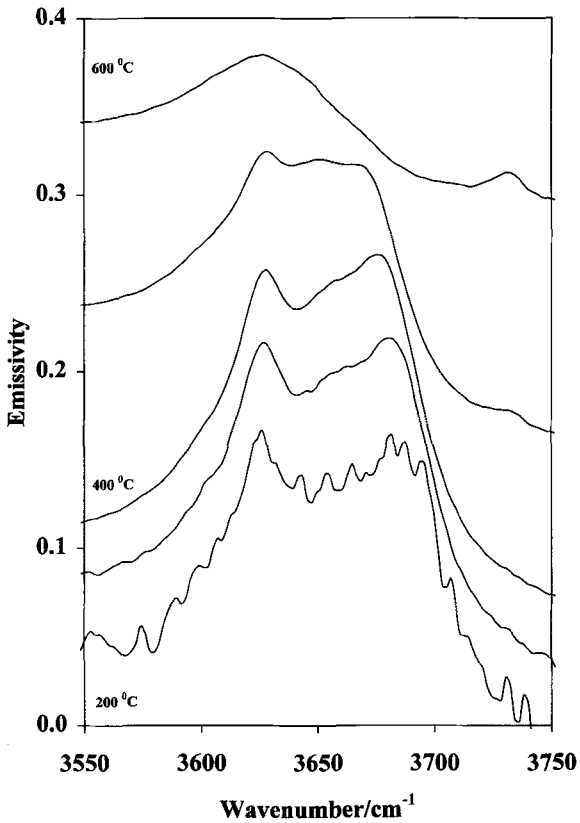

Figure 14. The IES of Eureka (Utah) Halloysite hydroxyls over the 200 to 600 °C range.

CONCLUSIONS

Infrared emission spectroscopy has been shown to be a very useful spectroscopic technique in the study of the dehydroxylation of the kaolinite clay minerals. The IES spectra clearly show the temperature at which dehydroxylation commences and the temperature at which it is complete. The spectra clearly illustrate those vibrations that involve Al-O and those that involve Si-O. The Si-O vibrations remain unchanged upon thermal treatment, whereas those involving Al-O undergo dramatic change on heating. The IES spectra clearly show the bands, which are due to vibrations not involving the hydroxyl groups. These bands remain unchanged throughout the heating process. For the kaolinites, the different clay hydroxyls were shown to be progressively removed simultaneously. It is proposed that the dehydroxylation of kaolinite takes place homogenously but in 2 steps that involve 2 separate mechanisms. In contrast, in dickite and halloysite the hydroxyls were removed at different rates as the temperature increased. The outer hydroxyl groups were

https://doi.org/10.1346/CCMN.1996.0440506 Published online by Cambridge University Press

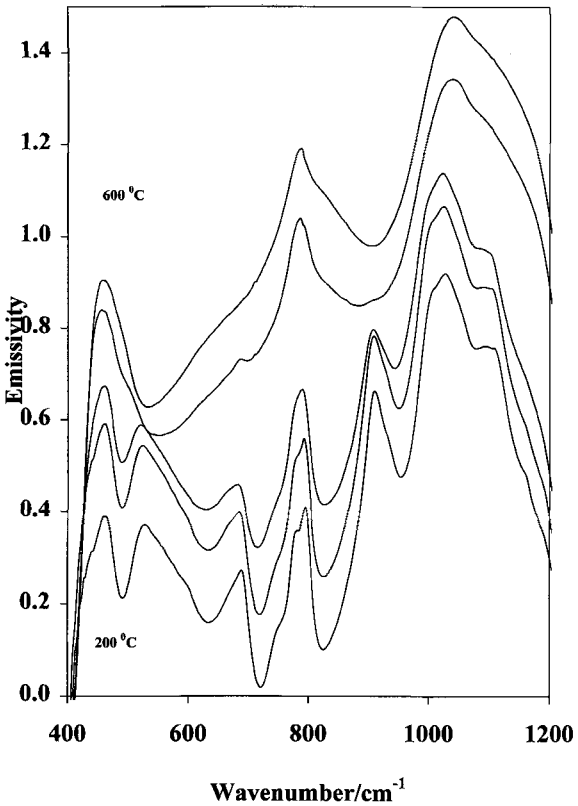

Figure 15. The IES of New Zealand Halloysite lattice region over the 200 to 600 °C range.

removed first. Spectroscopic evidence is provided for the existence of a new hydroxyl group formed at elevated temperatures during the dehydroxylation process of halloysite and dickite. This new peak is attributed to the formation of a silanol group which is formed during the dehydroxylation process. This new OH group is evidence that the dehydroxylation of the 2 clay minerals dickite and halloysite is taking place inhomogenously. Importantly the IES provides evidence that all 3 minerals dehydroxylate by different mechanisms. Kaolinite dehydroxylation differs from that of both dickite and halloysite.

REFERENCES

Axelson DE. 1987. ^{27}Al and ^{29}Si solid state nuclear magnetic resonance of coal and heavy oil-derived mineral matter. Fuel Sci Technol Int 5:561–92.

Ball MC, Taylor HFW. 1961. Dehydration of Brucite. Mineral Mag 32:754–766.

Bish DL, Johnston CT. 1993. Reitfeld refinement and Fourier Transform Infrared Spectroscopic Study of the Dickite Structure at Low Temperatures. Clays Clay Miner 41:297–304.

Brindley GW. 1961. Role of crystal structure in the dehydration reactions of some layer-type minerals. J Miner Soc Japan 5:217–237.

Brindley GW. 1963. Crystallographic aspects of some decomposition and recrystallisation reactions. Prog Ceram Sci 3:3–55.

Brindley GW. 1976. Aspects of layer stacking order in clays and layer silicates. Seventh Conference on clay mineralogy and petrology, Karlovy Vary. p 13–24.

Brindley GW, Chih-Chun K, Harrison JL, Lipsiscas M, Raythatha R. 1986. Relation between the structural disorder and other characteristics of kaolinites and dickites. Clays Clay Miner 34:233–249.

Brindley GW, Lemaitre J. 1987. Thermal, oxidation and reduction of clay minerals. In: Newman ACD, editor. Chemistry of clay and clay minerals. Essex, England: Longman Scientific and Technical. 319–370.

Brindley GW, Porter ARD. 1978. Occurrence of Dickite in Jamaica: Ordered and disordered varieties. Am Miner 63: 554–562.

Brindley GW, Sharp JH, Patterson JH, Achar BN, Narahari. 1967. Kinetics and mechanism of dehydroxylation processes. I. Temperature and vapour pressure dependence of dehydroxylation of kaolinite. Am Mineral 52:201–211.

Brindley GW, Suzuki T, Thiry M. 1983. Interstratified kaolinite/smectite from the Paris Basin: Correlations of layer proportions, chemical compositions and other data. Bull Mineral 106:403–410.

Brindley GW, Wan H. 1978. The 14 Å phase developed in heated dickites. Clay Miner 13:17–24.

Chakraborty, Akshoy K. 1992. Resolution of thermal peaks of kaolinite in thermomechanical analysis and differential thermal analysis studies. J Am Ceram Soc 75:2013–2016.

Collins DR, Fitch AN, Catlow C, Richard A. 1991. Time-resolved powder neutron diffraction study of thermal reactions in clay minerals. J Mater Chem 1:965–970.

Criado JM, Ortega A, Real C, Torres de Torres E. 1986. Effect of experimental conditions and particle size on the thermal dehydroxylation of kaolinite in a linear heating program. Bol Soc Esp Ceram Vidrio 25:299–305.

Davies TW, Hooper RM. 1985. Structural changes in kaolinite caused by rapid dehydroxylation. J Mater Sci Lett 4: 39–42.

Farmer VC. 1974. The layer silicates (Ch 15). In: Farmer VC, editor. The infrared spectra of minerals. London: Mineralogical Society. p 331–363.

Farmer VC, Russell JD. 1964. The infrared spectra of layered silicates. Spectrochimica Acta 20:1149–1173.

Friesen WI, Michaelian KH. 1986. Fourier Deconvolution of photoacoustic FTIR spectra. Infrared Phys 26:235–239.

Fripiat JJ, Toussaint F. 1960. Predehydroxylation state of kaolinite. Nature 186:627–628.

Fripiat JJ, Toussaint F. 1963. Dehydroxylation of kaolinite II conductometric measurements and infrared spectroscopy. J Phys Chem 67:30–36.

Frost RL. 1995. Fourier Transform Raman Spectroscopy of kaolinite, dickite and halloysite. Clays Clay Miner 43:191–195.

Frost RL, Bartlett JR, Fredericks PM. 1993. Fourier Transform Raman spectra of kandite clays. Spectrochim Acta 49A:667–674.

Frost RL, Finnie K, Collins B, Vassallo MJ. 1995. Infrared emission spectroscopy of clay minerals and their thermal transformations. In: Fitzpatrick RW, Churchman GJ, Eggleton T, editors. The Proceedings of the 10th International Clay Conference. Adelaide, Australia: CSIRO Publications. p 219–224.

Guggenheim S, van Groos AFK. 1992. High-pressure differential thermal analysis (HP-DTA). II. Dehydroxylation reactions at elevated pressures phyllosilicates. J Therm Anal 38:2529–2548.

Han X, Chen K. 1982. Infrared absorption spectra of minerals of the kaolinite-halloysite series. Dizhi Kexue 1:71–79.

Holdridge DA, Vaughan F. 1957. The kaolin minerals (Ch 4). In: Mackenzie RC, editor. The differential thermal investigation of clays. London: The Mineralogical Society. p 123–125.

Horvath I. 1985. Kinetics and compensation effect in kaolinite dehydroxylation. Thermochim Acta 85:193–8.

Jalajakumari B, Warrier KGK, Satyanarayana KG. 1989. Thermal dehydroxylation in surface modified kaolinite. J Mater Sci 24:2653–9.

Johnson SL, Guggenheim S, van Groos AFK. 1990. Thermal stability of halloysite by high-pressure differential thermal analysis. Clays Clay Miner 38:477–84.

Johnston CT, Agnew SF, Bish DL. 1990. Polarised single crystal Fourier-transform infrared microscopy of Ouray dickite and Keokuk kaolinite. Clays Clay Miner 38:573–583.

Johnston CT, Sposito G, Birge RR. 1985. Raman spectroscopic study of kaolinite in aqueous suspension. Clays Clay Miner 33:483–489.

Kristof J, Mink J, Horvath E, Gabor M. 1993. Intercalation study of clay minerals by Fourier transform infrared spectrometry. Vib Spectros 5:61–73.

Lambert JF, Millman WS, Fripiat JJ. 1989. Revisiting kaolinite dehydroxylation: A silicon-29 and aluminium-27 MAS NMR study. J Am Chem Soc 111:3517–22.

La Iglesia A. 1993. Pressure-induced disorder in kaolinite. Clay Miner 28:311–9.

Lazarev AN. 1972. Vibrational spectra and structure of silicates. New York: Plenum Press. p 178–182.

Ledoux RL, White JL. 1964. Infrared study of selective deuteration of kaolinite and halloysite at room temperature. Science 145:47–49.

Levy JH, Hurst HJ. 1993. Kinetics of dehydroxylation, in nitrogen and water vapor, of kaolinite and smectite from Australian Tertiary oil shales. Fuel 72:873–877.

Levy JH. 1990. Effect of water vapor pressure on the dehydration and dehydroxylation of kaolinite and smectite isolated from Australian tertiary oil shales. Energy Fuels 4: 146–151.

Mackenzie KJD. 1973. Simple high-temperature infrared cell and its application to the dehydroxylation of kaolinite. J Appl Chem Biotechnol 23:903–908.

Maiti GC, Freund F. 1981. Dehydration-related proton conductivity in kaolinite. Clay Miner 16:395–413.

Meinhold RH, Atakul H, Davies TW, Slade RCT. 1992. Flash calcination of kaolinite studied by DSC, TG and MAS NMR. J Therm Anal 38:2053–65.

Meinhold RH, Slade RCT, Davies TW. 1993. High-field aluminium-27 MAS NMR studies of the formation of metakaolinite by flash calcination of kaolinite. Appl Magn Reson 4:141–55.

Michaelian KH, Bukka K, Permann DNS. 1987. Photoacoustic infrared spectra (250–10,000 cm^{-1}) of partially deuterated kaolinite. Can J Chem 65:1420–1423.

Murat M, Chbihi MEM, Mathurin D. 1976. Heat of solution of different kaolinites and metakaolinites in hydrofluoric acid. Effect of crystal-chemical characteristics. Ind Ceram (Paris) 822:799–801.

Murata M, Mathurin D, Driouche M, Bachiorrini A. 1990. Investigations on some structural and physico-chemical properties of metakaolinite. Sci Geol Bull 43:213–223.

Ogloza AA, Malhotra VM. 1989. Dehydroxylation induced structural transformations in montmorillonite: An isothermal FTIR study. Phys Chem Miner 16:379–385.

Ohta K, Venkatesan MI. 1992. Pyrolysis of wood specimens with and without minerals: Implications to lignin diagenesis. Energy Fuels 6:271–277.

Pajcini V, Dhamelincourt P. 1994. Raman study of the OH-stretching vibrations in kaolinite at low temperature. Appl Spectrosc 48:638–641.

Pampuch R. 1971. Le Mechanisme de la deshydroxylation des hydroxides et des silicates phylliteux. Bull Groupe Fr Argiles 23:107–118.

Pampuch R. 1973. Applying IR spectroscopy to thermal decomposition of hydroxides and phyllosilicates. In: Boldyrev V, Meyer K, editors. Festkoerperchemie. Leipzig, East Germany Verlag Grundstoffind. p179–93.

Patterson JH, Hurst HJ, Levy JH, Killingley JS. 1990. Mineral reactions in the processing of Australian Tertiary oil shales. Fuel 69:1119–1123.

Petzold D, Poppe B, Trager T. 1985. Calorimetric determination of the dehydroxylation enthalpy of kaolinite. Silikattechnik 36:352–4.

Prost R, Damene AS, Huard E, Driard J, Leydecker JP. 1989. Infrared study of structural OH in kaolinite, dickite and nacrite and poorly crystalline kaolinite at 5 to 600K. Clays Clay Miner 37:464–468.

Prost R, Damene A, Huard E, Driard J. 1987. Infrared study of structural OH in kaolinite, dickite and nacrite at 300 to 5K. In: Schutz LG, van Olphen H, Mumpton FA, editors. Proceedings of the International Clay Conference, Denver. p 17–23.

Qiu X, Zhang Q. 1992. Measurement of mechanochemical changes of kaolin during dry fine grinding. Huanan Ligong Daxue Xuebao, Ziran Kexueban 20:145–52.

Redfern SAT. 1987. The kinetics of dehydroxylation of kaolinite. Clay Miner 22:447–56.

Rocha J, Adams JM, Klinowski J. 1990. The rehydration of metakaolinite to kaolinite: Evidence from solid state NMR and cognate techniques. J Sol State Chem 89:260–274.

Rocha J, Klinowski J. 1990. Silicon-29 and aluminium-27 magic-angle-spinning NMR studies of the thermal transformation of kaolinite. Phys Chem Miner 17:179–86.

Rocha J, Klinowski J, Adams JM. 1991. Solid-state NMR elucidation of the role of mineralizers in the thermal stability and phase transformations of kaolinite. J Mater Sci 26:3009–18.

Rouxhet PG, Samudacheata N, Jacobs H, Anton O. 1977. Attribution of the OH stretching bands of kaolinite. Clay Miner 12:171–178.

Roy R, Brindley GW. 1956. Hydrothermal reconstruction of the kaolin clay minerals. Clays Clay Miner 4:125–132.

Rue JW, Ott WR. 1974. Scanning electron microscopic interpretation of the thermal analysis of kaolinite. J Therm Anal 6:513–519.

Slade RCT, Davies TW, Atakul H. 1991. Flash calcination of kaolinite mechanistic information from thermogravimetry. J Mater Chem 1:751–756.

Slade RCT, Davies TW. 1989. The mechanism of kaolinite dehydroxylation followed by high resolution aluminium-27 and silicon-29 NMR. Coll Surf 36:119–25.

Stoch L, Waclawska I. 1981a. Dehydroxylation of kaolinite group minerals. I. Kinetics of dehydroxylation of kaolinite and halloysite. J Therm Anal 20:291–304.

Stoch L, Waclawska I. 1981b. Dehydroxylation of kaolinite group minerals. II. Kinetics of dickite dehydroxylation. J Therm Anal 20:305–310.

Stoch L. 1964. Thermal dehydroxylation of minerals of the kaolinite group. Bull Acad Polonaise Sci 12:173–180.

Stubican V, Roy R. 1961. Proton retention in heated 1:1 clays studied by infrared spectroscopy, weight loss and deuterium uptake. J Phys Chem 65:1348–1351.

Taranukhina LD, Paukstis E, Goncharuk VV. 1991. Quantitative study of the proton acidity of natural aluminosilicates by IR spectroscopic method. Z Prikl Khim (St.-Petersburg) 64:2633–6.

Tarasevich YI, Gribina IA. 1985. State of structural hydroxyl groups in minerals of the kaolinite group according to IR spectroscopy data. Teor Eksp Khim 21:73–81.

Toussaint F, Fripiat JJ, Gastuche MC. 1963. Dehydroxylation of kaolinite I. Kinetics. J Phys Chem 67:26–29.

Van der Marel HW, Krohmer P. 1976. Beitr Mineral Petrol 22:73–82.

Vassallo AM, Cole-Clarke PA, Pang LSK, Palmisano A. 1992. Infrared Emission spectroscopy of coal minerals and their thermal transformations. J Appl Spectrosc 46:73–78.

Wada K. 1967. A study of hydroxyl groups in kaolin minerals utilising selective deuteration and infrared spectroscopy. Clay Miner 7:51–61.

White JL, Laycock A, Cruz, M. 1970. Infrared studies of proton delocalization in kaolinite. Bull Groupe Fr Argiles 22:157–165.

Yeskis D, van Groos AFK, Guggenheim S. 1985. The dehydroxylation of kaolinite. Am Mineral 70:159–64.

Zhang Z, Yuan R. 1993. Dehydroxylation process of kaolinite and its structural change. Guisuanyan Tongbao 12:37–41.

(Received 5 May 1995; accepted 29 December 1995; Ms. 2647)